The American Journal of Engineering and Technology
(ISSN – 2689-0984)
VOLUME 04 ISSUE 04 Pages: 17-35
SJIF IMPACT FACTOR (2020: 5. 32) (2021: 5. 705) (2022: 6. 456)
OCLC – 1121105677 METADATA IF – 7.856
Publisher: The USA Journals

Journal Website: https://theamericanjournals.com/index.php/tajet

Research Article

COMPARISON OF MPPT ALGORITHMS FOR PV SYSTEM USING SINGLE DIODE AND THEVENIN EQUIVALENT MODELS

Submission Date: April 05, 2022, **Accepted Date:** April 15, 2022,
Published Date: April 28, 2022 |
Crossref doi: https://doi.org/10.37547/tajet/Volume04Issue04-03

Ali Haider Dahash
Al-Nahrain University College of Engineering Electronic and Communications Engineering, Iraq

Anas Lateef Mahmood
Al-Nahrain University College of Engineering Electronic and Communications Engineering, Iraq

ABSTRACT

Maximum Power Point Tracking (MPPT) algorithms are significant in PV systems due to they reduce the PV panels number that necessary to reach the target output power, lowering the PV array expense. This research gives a simulated comparison of two essential MPPT techniques, incremental conductance (IC) and perturb and observe (P&O) utilizing single diode and Thevenin comparable models. The essential parameters involving voltage, current, and power output were traced for both methods using a DC-DC boost converter. The results of stimulation revealed that for the two tracking algorithms the single diode module gives higher output power in comparison with the Thevenin equivalent model but for the IC algorithm the Thevenin equivalent model gives less output signals ripple.

KEYWORDS

Photovoltaic (PV), Maximum Power Point Tracking (MPPT), Perturb and Observe (P&O), Incremental Conductance (IC).

The American Journal of Engineering and Technology
(ISSN – 2689-0984)
VOLUME 04 ISSUE 04 Pages: 17-35
SJIF IMPACT FACTOR (2020: 5. 32) (2021: 5. 705) (2022: 6. 456)
OCLC – 1121105677 METADATA IF – 7.856
Publisher: The USA Journals

INTRODUCTION

Photovoltaic (PV) generating is among the most promising renewable green energy resource right now. PV generating is favoured above other renewable energy sources due to its environmental and economic benefits, as it is clean, infinite, and requires no maintenance. PV cells produce electricity by altering solar energy directly into electrical energy. The panels of PV and arrays provide direct current (DC) power that must be transformed to alternating current (AC) at a standard power frequency for the purpose of power loads. As a result, between the PV arrays and the grid, power converters are required [1]. Grid-connected inverters can transfer photovoltaic energy to power system networks. One key issue with PV systems is the possible mismatch with the operational parameters of the PV array and the load. As a PV array is directly linked to a load, the operational point of the system is at the intersection of the I-V curves of the load and the PV array. Most of the time, the Maximum Power Point (MPP) of a PV array is not reached. This issue is solved by usage an MPPT that keeps the PV array's operational point at the MPP. Because the occurrence of MPP in the I-V plane was unknown previously, it was determined utilizing a PV array model and calculations of array temperature and irradiance. Measurements these data is frequently prohibitively high-priced, and the essential parameters for the PV array model are not well understood. As a result, the MPPT is constantly looking for MPP. Many MPPT continuously searches algorithms have been presented, each of which takes into account various properties of solar panels and the placement of the MPP [2, 3]. A MPPT is utilized to excerpt the greatest power from the solar PV module then send this power to the load. A dc/dc converter (step up/step down) is a device that transmits maximum power from a solar PV module to a load and serves as an interfacing of the module with the load. When the duty cycle is modified, the maximum power is transported via altering the impedance of the load as observed by the source and matching it at the highest power of it. Different MPPT strategies are necessary to keep PV arrays working at their MPP. A lot of MPPT strategies are suggested in the paper, including the the Incremental Conductance (IC) method, Perturb and Observe (P&O) method, the Fuzzy Logic Method, and others [4, 5]. The two most widely utilized MPPT strategies (Perturb and Observe (P&O) and Incremental Conductance (IC) procedures) are investigated [6]. The following is how the research is organized. Section 2 discusses the fundamental principle of a PV cell as well as the properties of (Mathematical model PV array) and (Thevenin equivalent model for a PV source). Section 3 describes in detail the P&O and IC MPPT algorithms. Section 4 discusses the results of the simulation (single diode model PV array) and (Thevenin equivalent model for a PV source), MPPT methods, and their comparison.

2. PV ARRAY CHARACTERISTICS

2.1 PV Cell fundamental Principle

PV cells are basically p-n junction diodes with a relatively large area formed by constructing a junction between the p-type and n-type regions. When sunlight reaches a PV cell, it is transformed immediately into electrical energy. Within the semiconductor the energy from the transmitted light is utilized to activate free electrons from a low energy state to an unoccupied higher energy level. When a PV cell is activated, light generates extra electron-hold pairs across the material, shortening the p-n junction and allowing current to flow.

2.2 PV Array (Single Diode Model) Properties

The American Journal of Engineering and Technology
(ISSN – 2689-0984)
VOLUME 04 ISSUE 04 Pages: 17-35
SJIF IMPACT FACTOR (2020: 5. 32) (2021: 5. 705) (2022: 6. 456)
OCLC – 1121105677 METADATA IF – 7.856
Publisher: The USA Journals

The single diode model for PV, as explained in Figure 1, consists of a current source represent the photogenerated current, a diode, and two resistances (series and parallel). The output current can be calculated using Kirchhoff's current law and written as in (1) [7-9].

$$I = I_{ph} - I_0\left\{exp\left(\frac{V+IR_s}{n_sV_t}\right) - 1\right\} - \frac{V+IR_s}{R_{sh}} \quad (1)$$

where I and V represent the module output current and voltage respectively; Io and Iph represent the dark saturation current and photo-generated current respectively; while the junction thermal voltage is denoted by Vt, while the series and parallel resistances are denoted by Rs and Rsh, respectively. ns denotes the cells numbers in the module that are connected in series. The diode's thermal voltage is proportional to the junction temperature, as shown by (2),

$$V_t = \frac{kTA}{q} \quad (2)$$

where k denotes the Boltzmann constant, A denotes the diode quality factor, T is the junction temperature, and q denotes the electronic charge.

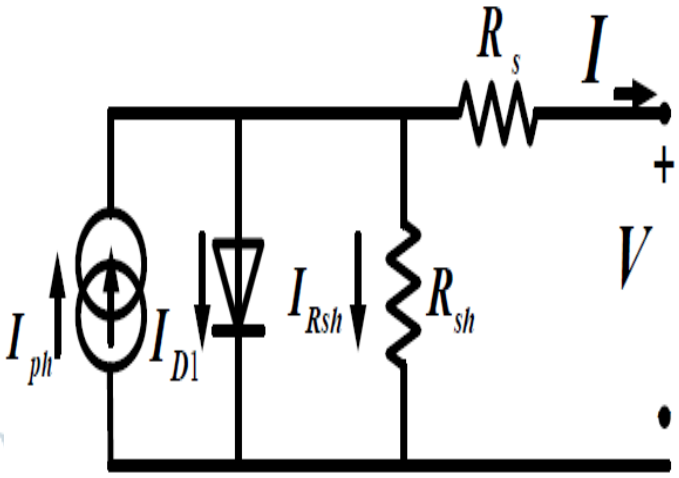

Fig. 1 A PV source with a single diode.

The single diode model has 5 undetermined parameters that must be calculated before building Thevenin's counterpart of the model. Iph, Io, VT, Rs, and Rsh are the unknown parameters. These parameters are estimated using the information from the manufacturer's datasheet. Once the parameters are determined, they are changed to account for changing environmental circumstances. After the parameters are determined, the model is linearized to gain Thevenin's equivalent model of PV as observed back into PV from its output terminals. Further articles on the subject can be found in [10-14]. As illustrated in Fig. 2, photovoltaic arrays have an optimum operating point known as the MPP. It is observed that power grows as elevation of voltage, reaching a peak value, then declines as resistance climbs to a point where current decline. Depending to the hypothesis of the maximum power transfer, this is the point at which the load is proportional to the resistance of the solar panel at a particular level of insolation and temperature [15].

The American Journal of Engineering and Technology
(ISSN – 2689-0984)
VOLUME 04 ISSUE 04 Pages: 17-35
SJIF IMPACT FACTOR (2020: 5. 32) (2021: 5. 705) (2022: 6. 456)
OCLC – 1121105677 METADATA IF – 7.856
Publisher: The USA Journals

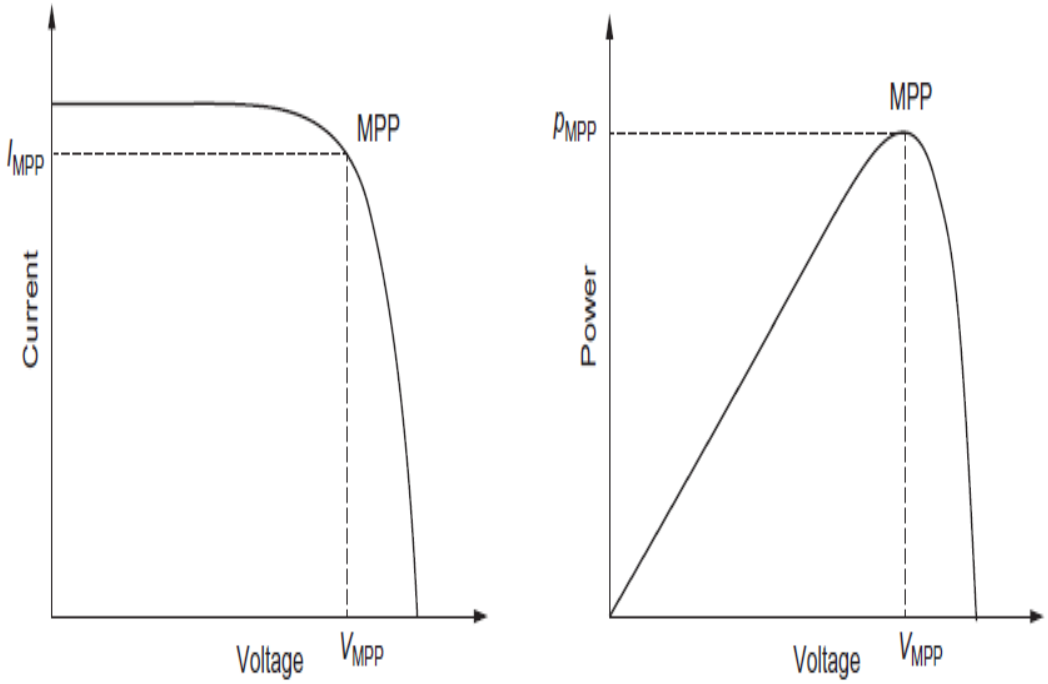

Fig. 2 Typical PV module curves: (A) I-V property of a solar cell displaying the MPP and (B) P-V property of a solar cell displaying the MPP [15].

Case Study

At STC (250C and 1000 W/m2), a case study was undertaken to determine the specifications of the PV array module generated using Mitsubishi Electric, PV-MF165EB3. Table 1 shows the numbers from the datasheet, then the unknown parameters was calculated.

The American Journal of Engineering and Technology
(ISSN – 2689-0984)
VOLUME 04 ISSUE 04 Pages: 17-35
SJIF IMPACT FACTOR (2020: 5. 32) (2021: 5. 705) (2022: 6. 456)
OCLC – 1121105677 METADATA IF – 7.856
Publisher: The USA Journals

Table 1 Module datasheet values and estimated parameters

Datasheet Values		Estimated Parameters	
I_{sc}	7.36 A	I_{ph}	7.36 A
V_{oc}	30.4 V	I_o	0.104 μA
V_{mpp}	24.2 V	A	1.310
I_{mpp}	6.83 A	R_s	0.251 ohm
n_s	50	R_{sh}	1168 ohm
Temperature coefficients			
K_i	0.057%	K_v	-0.346%

The PV array's mathematical model is created using the MATLAB Simulink toolbox, and the numerous equations characterizing the PV array's properties are modeled utilizing appropriate blocks from the Simulink library. Figure 3 depicts the entire Simulink model of the PV module, whereas Figure 4 depicts the I-V, P-V plot.

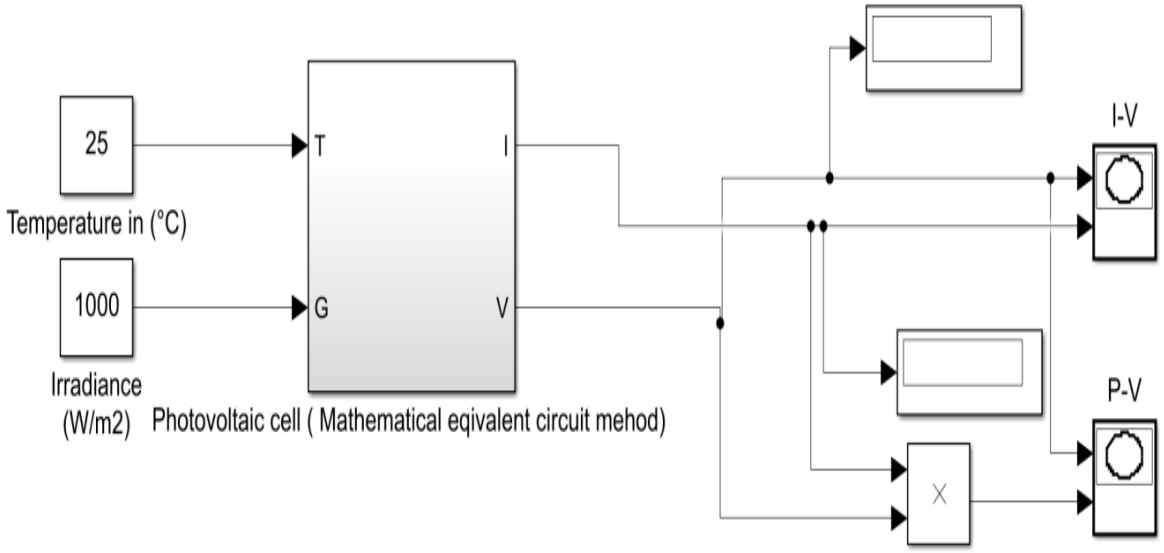

Fig. 3 Simulation model of the solar PV array model.

The American Journal of Engineering and Technology
(ISSN – 2689-0984)
VOLUME 04 ISSUE 04 Pages: 17-35
SJIF IMPACT FACTOR (2020: 5. 32) (2021: 5. 705) (2022: 6. 456)
OCLC – 1121105677 METADATA IF – 7.856
Publisher: The USA Journals

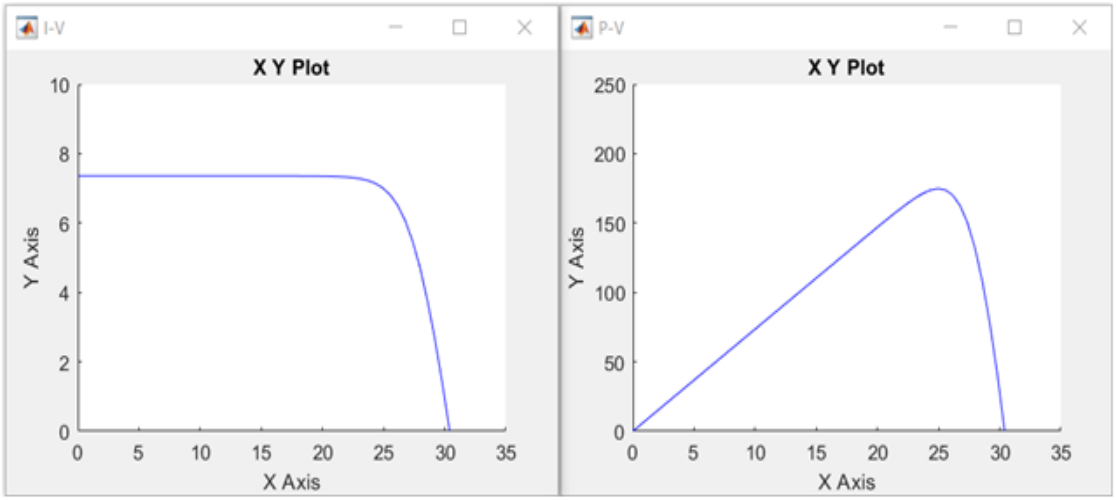

Fig. 4 I-V and P-V property for PV array model under STC (250C and 1000 W/m2)

2.3 Thevenin Equivalent Model for the Characteristics of a PV Source

$$I_D = I_o \left\{ exp\left(\frac{v_D}{n_s \cdot V_t}\right) - 1 \right\} \quad (3)$$

The sole non-linear element in the model is the diode. The current and voltage (I-V) in it are linked by an exponential correlation as directed by Shockley and is present in (3) [5]:

Where ID and VD are the diode current and voltage respectively.

As demonstrated in Figure 5, piecewise linearization is utilized to linearize the diode.

The American Journal of Engineering and Technology
(ISSN – 2689-0984)
VOLUME 04 ISSUE 04 Pages: 17-35
SJIF IMPACT FACTOR (2020: 5. 32) (2021: 5. 705) (2022: 6. 456)
OCLC – 1121105677 METADATA IF – 7.856
Publisher: The USA Journals

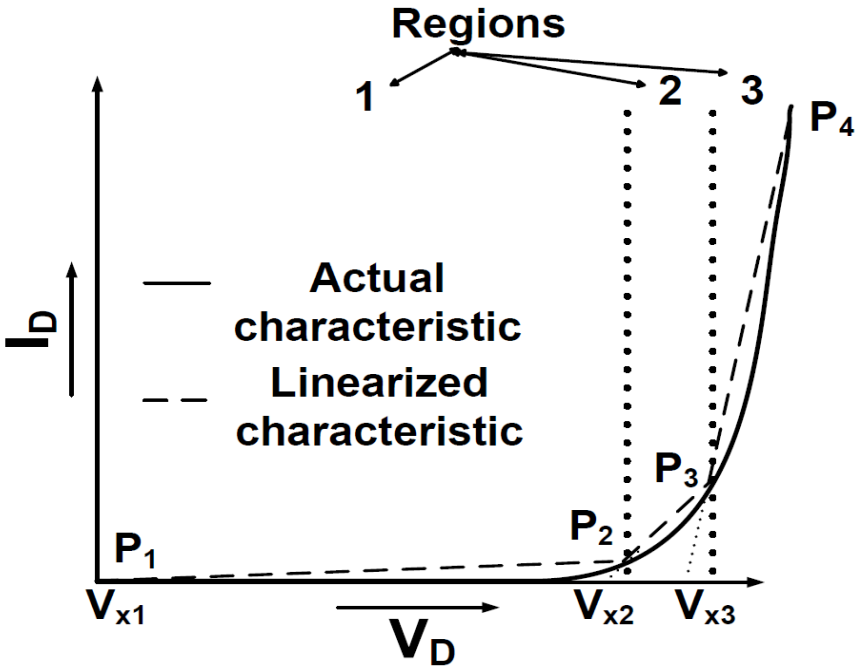

Fig. 5 A diode's voltage current characteristic, with actual and linear approximations [16].

Figure 6 depicts the PV model with the diode linearized. The values of RD and Vx will vary depending on the operating region.

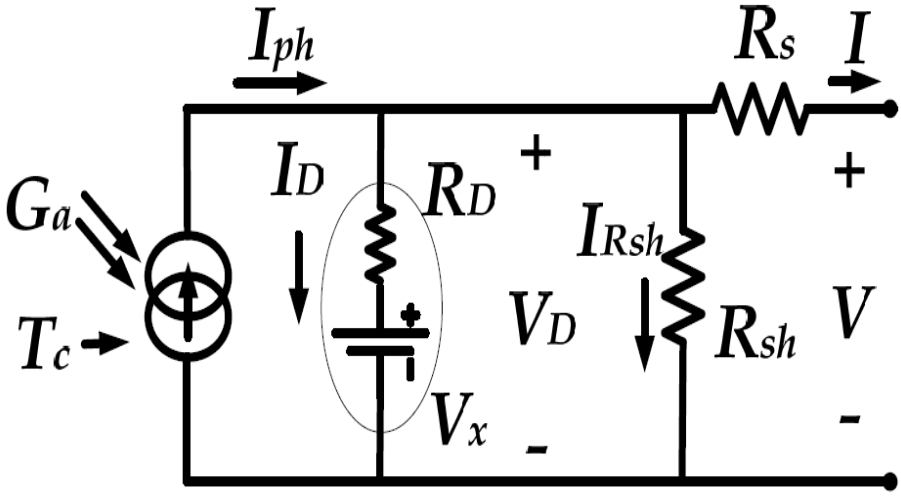

Fig. 6. PV model with linearized diode

The American Journal of Engineering and Technology
(ISSN – 2689-0984)
VOLUME 04 ISSUE 04 Pages: 17-35
SJIF IMPACT FACTOR (2020: 5. 32) (2021: 5. 705) (2022: 6. 456)
OCLC – 1121105677 METADATA IF – 7.856
Publisher: The USA Journals

In figure 6. Show the linearized model that can now be denoted by the resistance and voltage of Thevenin's equivalent given in (4) and (5):

$$V_{Th,i} = V_{x,i} + R_{D,i} \cdot \frac{I_{ph} \cdot R_{sh} - V_{x,i}}{R_{sh} + R_{D,i}} \quad (4)$$

$$R_{Th,i} = R_s + \frac{R_{sh} \cdot R_{D,i}}{R_{sh} + R_{D,i}} \quad (5)$$

Where VTh, i and RTh, i are the Thevenin's equivalent voltage and resistance of the model in figure 6 at region I = 1, 2,....number of regions). Figure 7 depicts PV as seen from its output terminals.

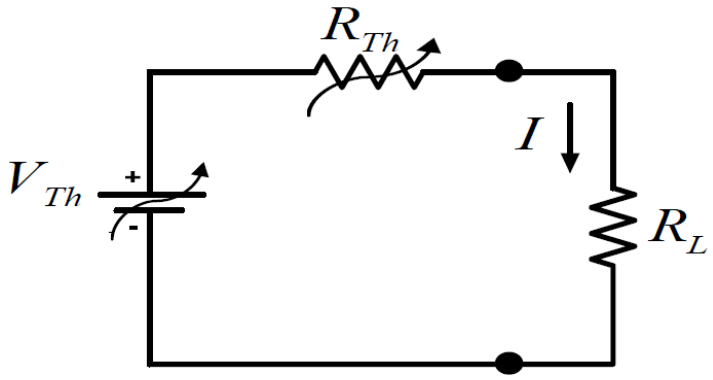

Fig. 7. PV Thevenin's equivalent circuit

Case Study

At STC and (250C and 1000 W/m2), a case study was undertaken to determine the specifications of the PV array module generated using Mitsubishi Electric, PV-MF165EB3. Table 2 shows the values from the datasheet, then the unknown parameters was calculated.

The American Journal of Engineering and Technology
(ISSN – 2689-0984)
VOLUME 04 ISSUE 04 Pages: 17-35
SJIF IMPACT FACTOR (2020: 5. 32) (2021: 5. 705) (2022: 6. 456)
OCLC – 1121105677 METADATA IF – 7.856
Publisher: The USA Journals

Table 2 Module datasheet values and estimated parameters

Datasheet Values		Estimated Parameters	
I_{sc}	7.36 A	I_{ph}	7.36 A
V_{oc}	30.4 V	I_o	0.104 μA
V_{mpp}	24.2 V	A	1.310
I_{mpp}	6.83 A	R_s	0.251 ohm
n_s	50	R_{sh}	1168 ohm
Temperature coefficients			
K_i	0.057%	K_v	-0.346%

Thevenin's equivalent model for a PV source is created utilizing the MATLAB Simulink toolbox. The numerous equations representing the PV properties of Thevenin's equivalent model are modeled utilizing appropriate blocks from the Simulink library and m-file codes. The entire Simulink model of the PV module is presented in Fig. 8, and the I-V and P-V plots are displayed in Fig. 9.

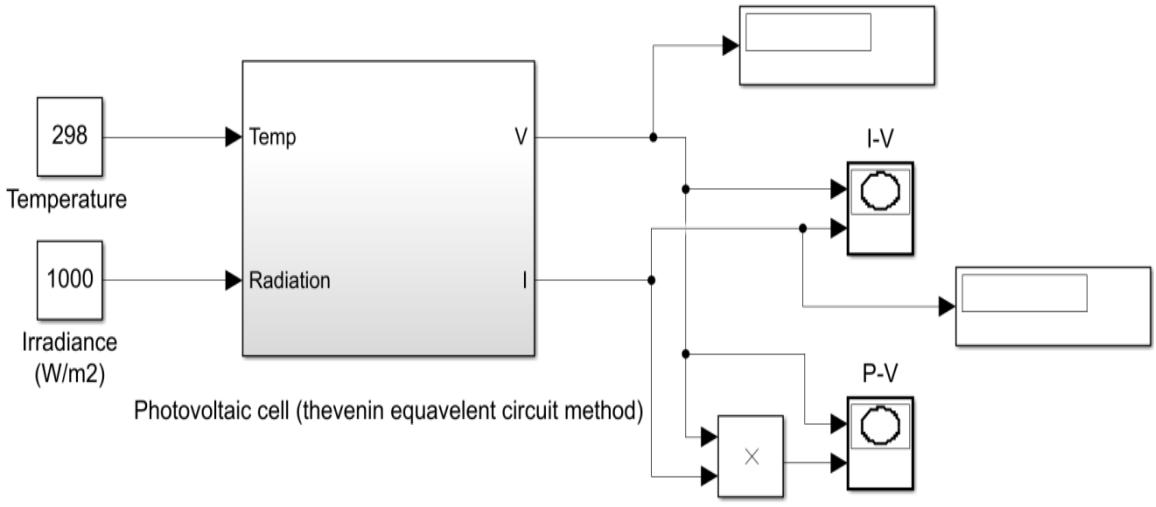

Fig. 8 Simulink for Thevenin's equivalent of photovoltaic source models

The American Journal of Engineering and Technology
(ISSN – 2689-0984)
VOLUME 04 ISSUE 04 Pages: 17-35
SJIF IMPACT FACTOR (2020: 5. 32) (2021: 5. 705) (2022: 6. 456)
OCLC – 1121105677 METADATA IF – 7.856
Publisher: The USA Journals

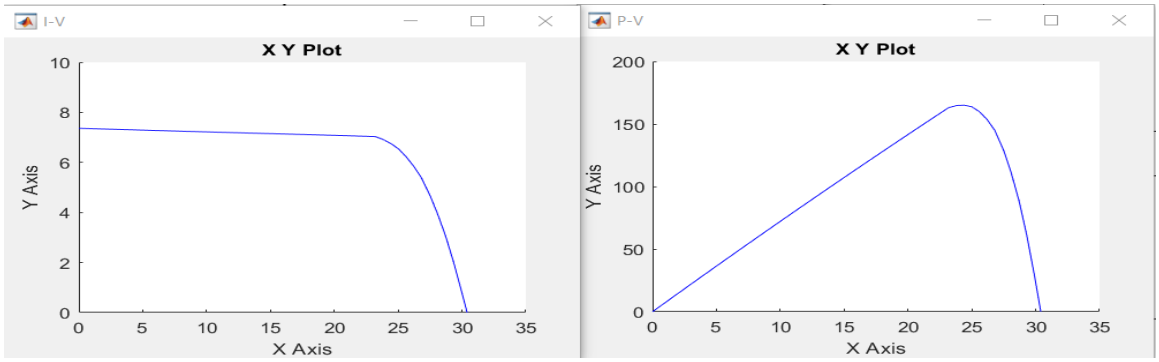

Fig. 9 plot I-V and P-V characteristic under STC (25oC and 1000 W/m2)

3. MPPT CONTROL ALGHORITHMS

3.1 Perturb and Observe Method

P&O is the most frequently utilized MPPT algorithm since it is easy to build in its citation form. Hence, if the operating voltage of the PV is perturbed in a certain direction and dP/dV > 0, as it is known that the perturbation shifted the array's operating point upon the MPP, then the algorithms of the P and O would continue to disturb the PV voltage in the same direction. If dP/dV = 0, the alter in operating point pulls the PV away from the MPP, and the P & O algorithm inverses the direction of the perturbation. P&O has an issue in that it oscillates about the MPP in steady-state operation. Under rapidly elevation or declining irradiance levels, it can also track in the other direction, away from the MPP [17]. Figure 10 depicts a simple flow chart of the P&O approach.

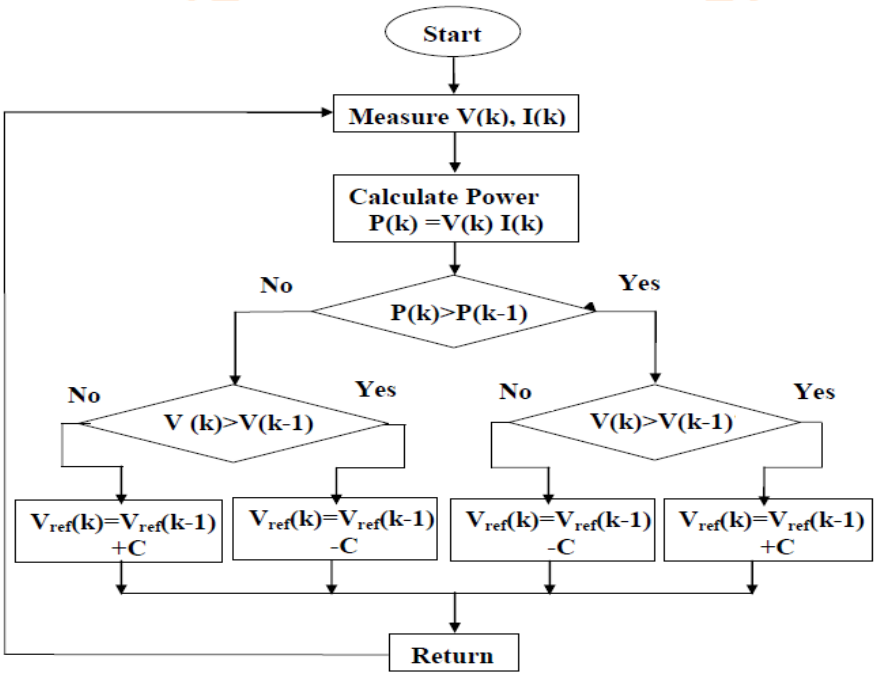

Fig. 10 P&O method flowchart [18].

The American Journal of Engineering and Technology
(ISSN – 2689-0984)
VOLUME 04 ISSUE 04 Pages: 17-35
SJIF IMPACT FACTOR (2020: 5. 32) (2021: 5. 705) (2022: 6. 456)
OCLC – 1121105677 METADATA IF – 7.856
Publisher: The USA Journals

3.2 IncCond Method (Incremental Conductance Method)

The IncCond approach attempts to circumvent the restrictions of the P&O technique by computing the sign of dP/dV without a perturbation usage the PV array's incremental conductance. The advantage of this approach over the P&O algorithm is that it can tell when the MPPT has achieved the MPP, while the P&O algorithm oscillates about the MPP. Furthermore, incremental conductance can trail quickly growing and falling irradiance circumstances with greater precision than P&O, which is unable to relate changes in PV power to changes in meteorological conditions. One downside of this technique is that it is more sophisticated than P&O, which increases processing time. Figure 11 [19, 20] depicts a simple flowchart for this strategy.

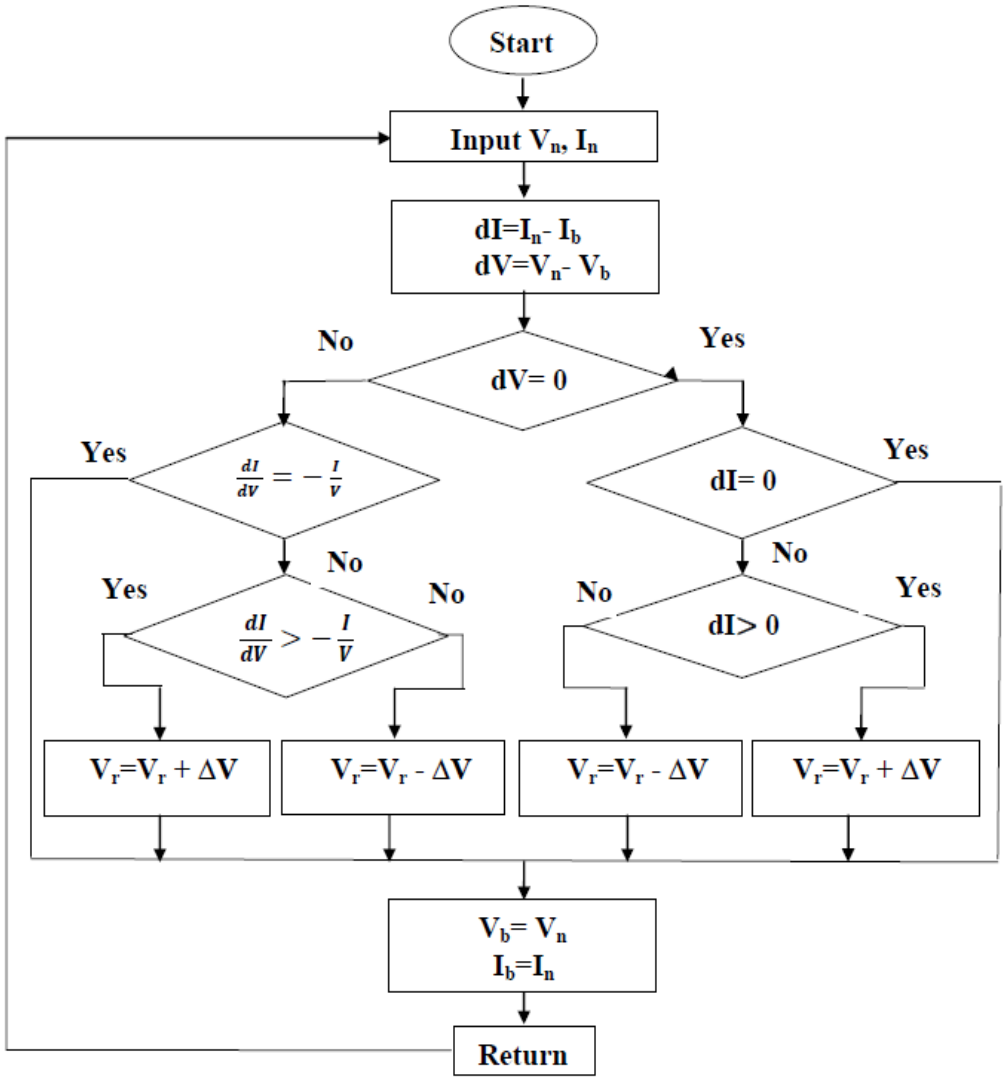

Fig. 11 Flowchart of IncCond algorithm [20].

The American Journal of Engineering and Technology
(ISSN – 2689-0984)
VOLUME 04 ISSUE 04 Pages: 17-35
SJIF IMPACT FACTOR (2020: 5. 32) (2021: 5. 705) (2022: 6. 456)
OCLC – 1121105677 METADATA IF – 7.856
Publisher: The USA Journals

4. Activation RESULTS AND DISCUSSIONS

4.1 Simulink Model of P&O and IC Algorithms

The PV array mathematical model is included in the MATLAB subsystem, as are the equations needed to model it. The DC voltage resource of the dc-dc boost converter was considered in the PV array mathematical model. The algorithms of the P&O and IC MPPT are utilized to calculate power at the operational point. Figure 12 depicts a Simulink model of a PV array with a dc-dc boost converter, as well as P&O and IC MPPT algorithms. Figure 13 depicts the simulation results of a comparison of IC and P&O MPPT algorithms, with the outputs of voltage, current, and power.

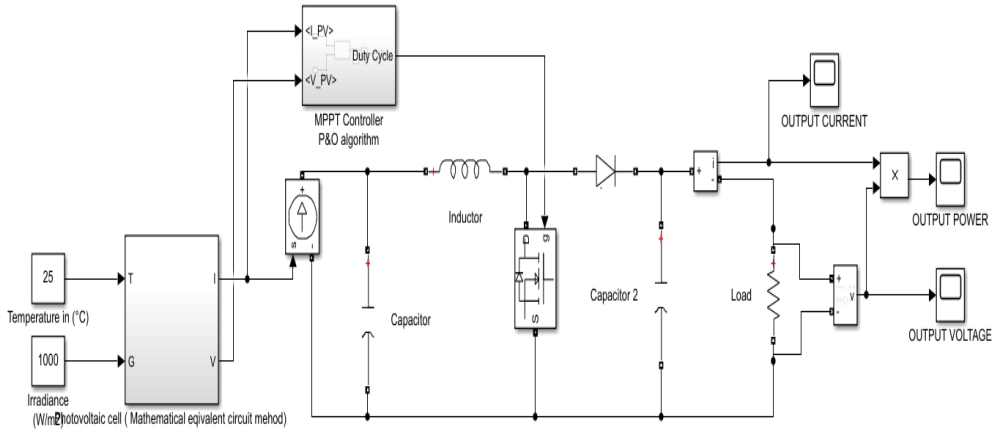

Figure (a) P&O MPPT algorithm

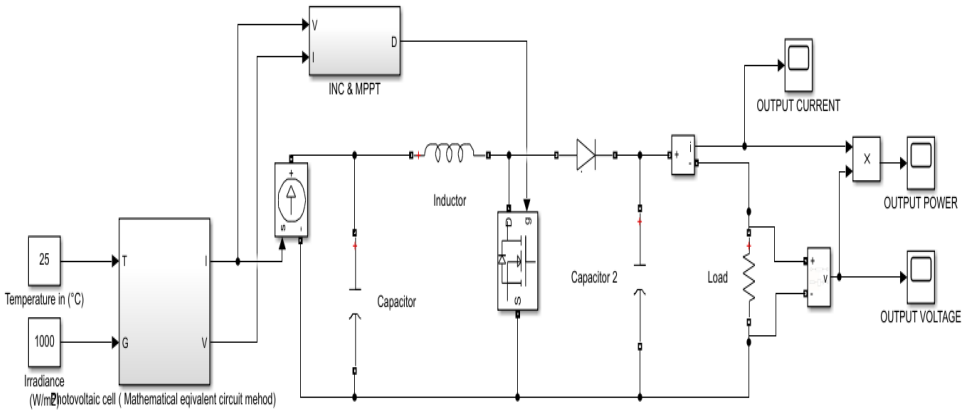

Figure (b) IC MPPT algorithm

Fig. 12 Simulink model of PV array with a dc-dc boost converter

The American Journal of Engineering and Technology
(ISSN – 2689-0984)
VOLUME 04 ISSUE 04 Pages: 17-35
SJIF IMPACT FACTOR (2020: 5. 32) (2021: 5. 705) (2022: 6. 456)
OCLC – 1121105677 METADATA IF – 7.856
Publisher: The USA Journals

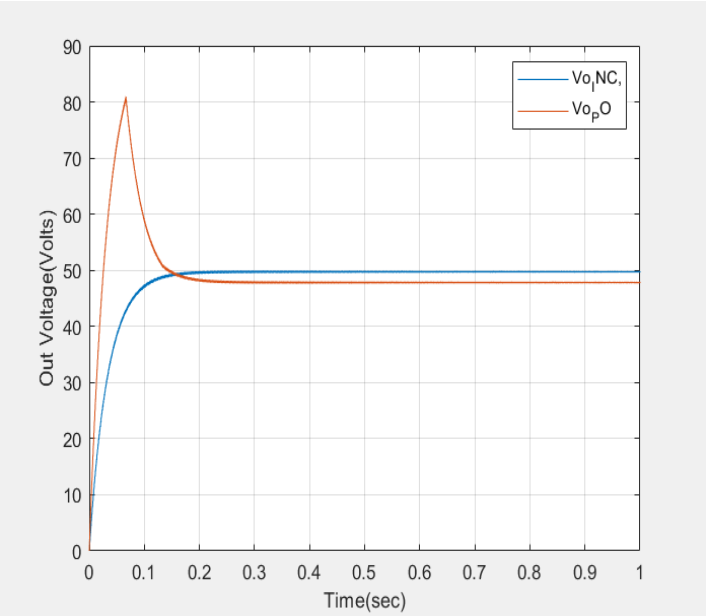

Figure (a) Output Voltage

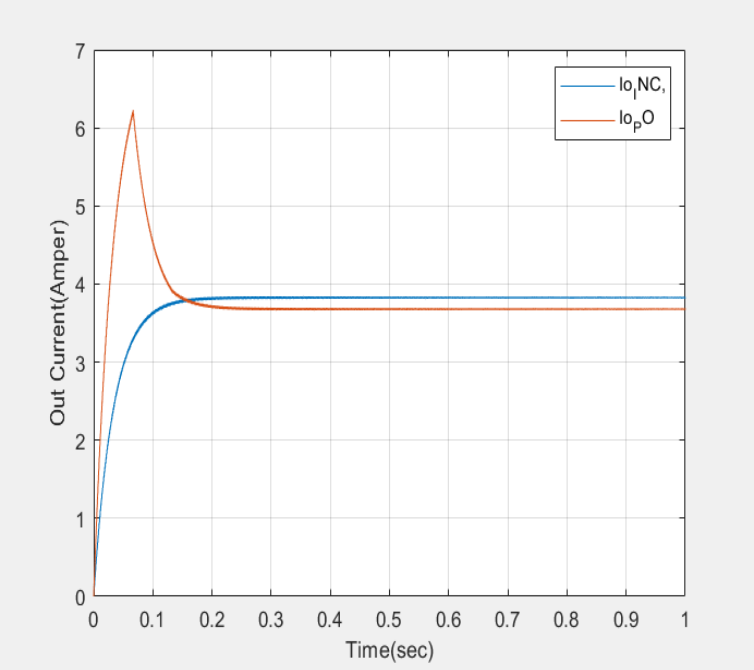

Figure (b) Output Current

The American Journal of Engineering and Technology
(ISSN – 2689-0984)
VOLUME 04 ISSUE 04 Pages: 17-35
SJIF IMPACT FACTOR (2020: 5. 32) (2021: 5. 705) (2022: 6. 456)
OCLC – 1121105677 METADATA IF – 7.856
Publisher: The USA Journals

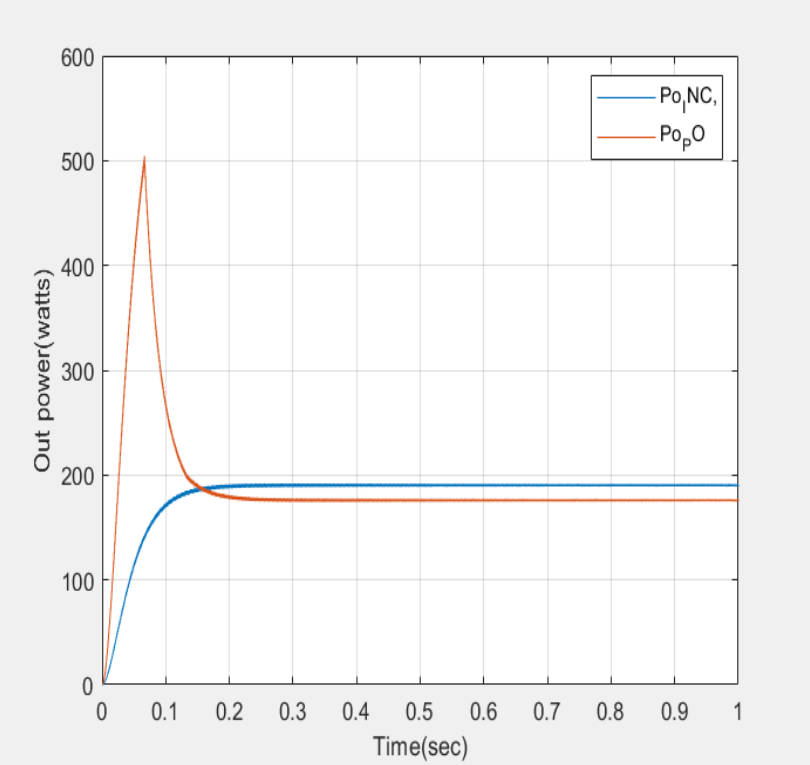

Figure (c) Output Power

Fig. 13 Activation results of the algorithms of P&O and IC MPPT

4.2 Comparison of P&O and IC MPPT Algorithms

Using the identical conditions (250C and 1000W/m2), the P&O and IC MPPT algorithms are activated and compared. Table 3 shows the results of the comparison of the P&O and IC MPPT algorithms.

Table 3 Comparison between P&O and IC algorithms for single diode model.

MPPT	Output Voltage	Output Current	Output Power	Ripple Voltage	Accuracy
P&O	47.9135	3.6883	176.763	0.24	Less
IC	49.7165	3.8274	190.907	0.315	Accurate

4.3 P&O and IC Algorithms Simulink Model

The PV of Thevenin's corresponding model attributes are represented by appropriate Simulink library blocks

The American Journal of Engineering and Technology
(ISSN – 2689-0984)
VOLUME 04 ISSUE 04 Pages: 17-35
SJIF IMPACT FACTOR (2020: 5. 32) (2021: 5. 705) (2022: 6. 456)
OCLC – 1121105677 METADATA IF – 7.856
Publisher: The USA Journals

and m-file codes. Figure 14 depicts a Simulink model of a PV array with a dc-dc boost converter, as well as P&O and IC MPPT algorithms. Figure 15 depicts the simulation results of a comparison of P&O and IC MPPT algorithms, with outputs of voltage, current, and power explained.

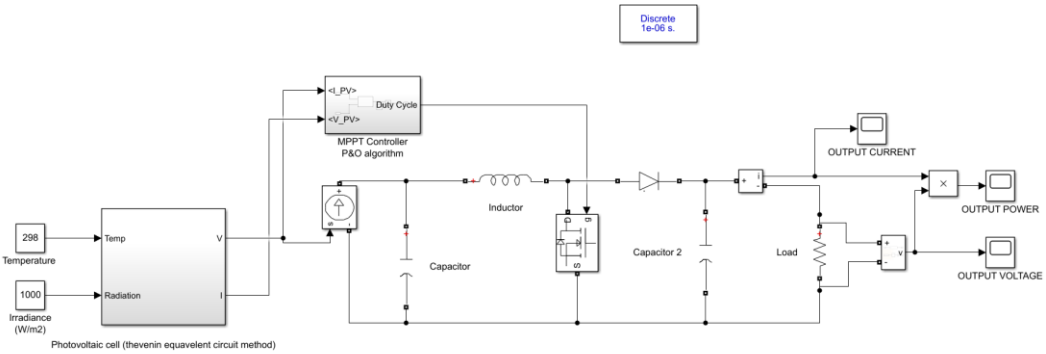

Figure (a) P&O MPPT algorithm

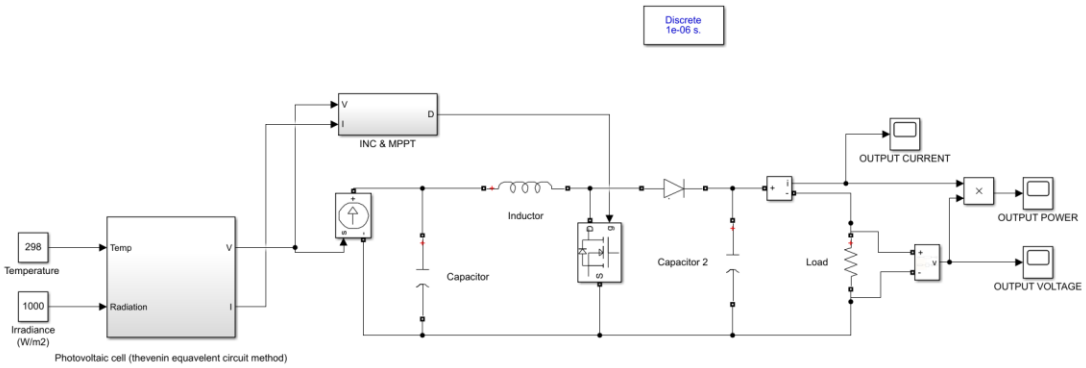

Figure (b) IC MPPT algorithm

Fig. 14 Thevenin's equivalent model for a PV source with a dc-dc boost converter

The American Journal of Engineering and Technology
(ISSN – 2689-0984)
VOLUME 04 ISSUE 04 Pages: 17-35
SJIF IMPACT FACTOR (2020: 5. 32) (2021: 5. 705) (2022: 6. 456)
OCLC – 1121105677 METADATA IF – 7.856
Publisher: The USA Journals

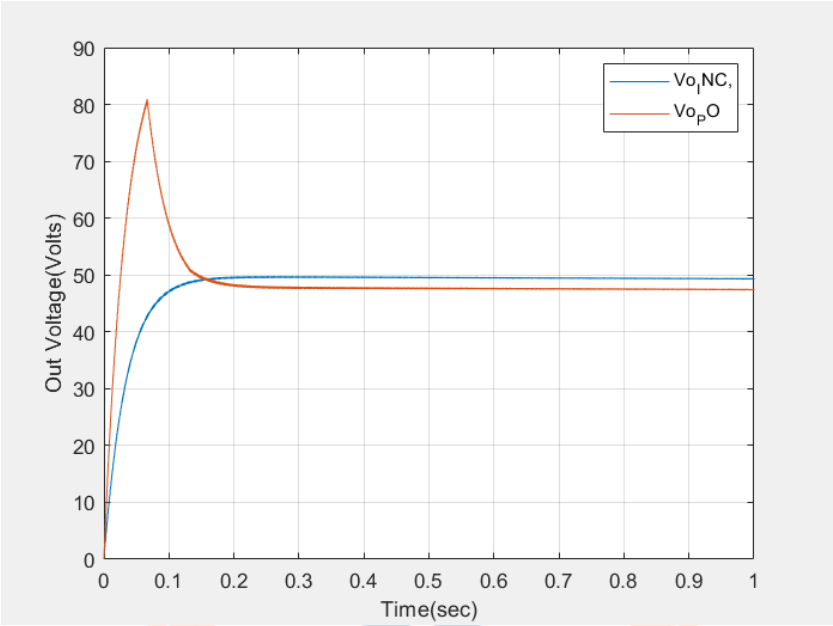

Figure (a) Output Voltage

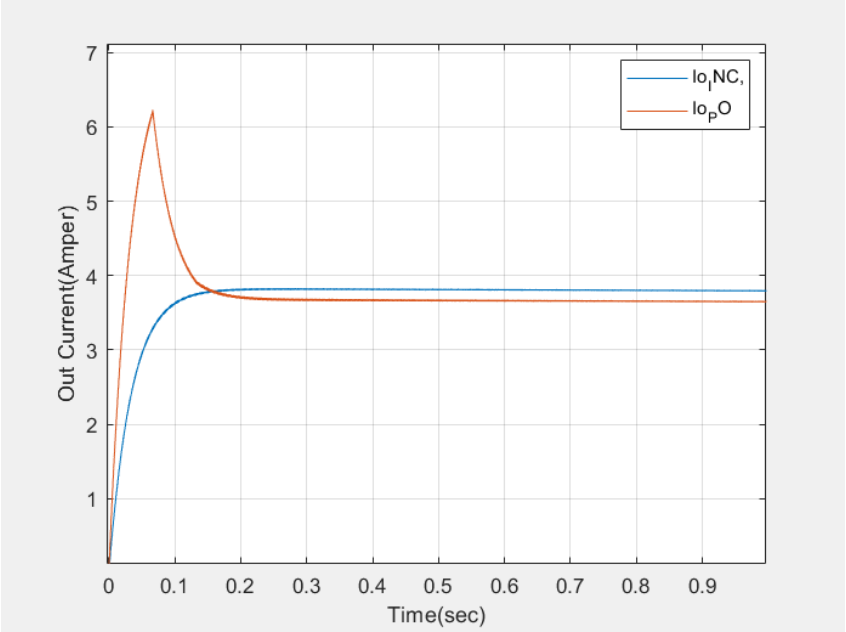

Figure (b) Output Current

The American Journal of Engineering and Technology
(ISSN – 2689-0984)
VOLUME 04 ISSUE 04 Pages: 17-35
SJIF IMPACT FACTOR (2020: 5. 32) (2021: 5. 705) (2022: 6. 456)
OCLC – 1121105677 METADATA IF – 7.856
Publisher: The USA Journals

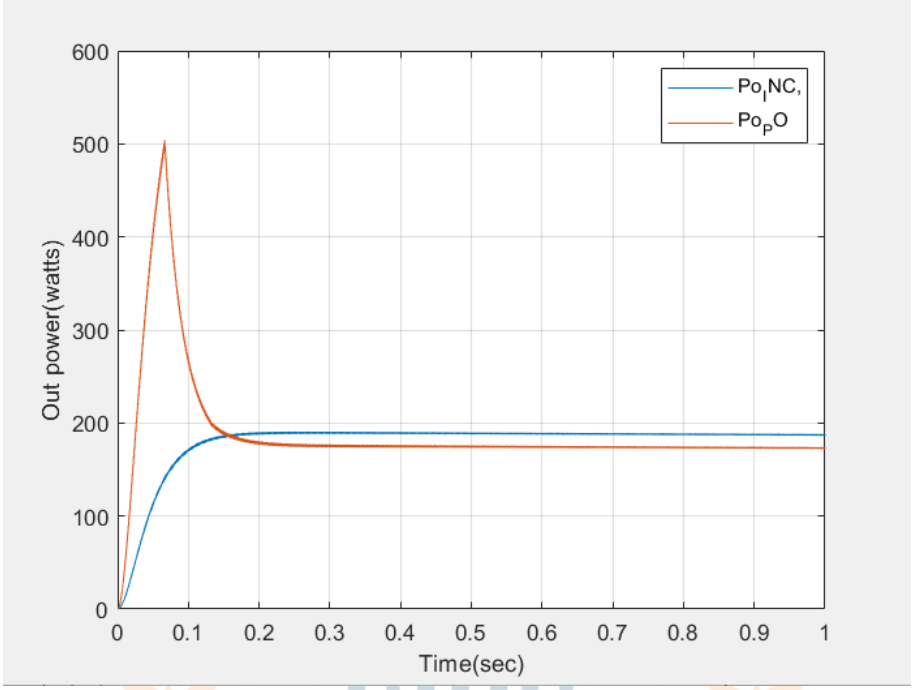

Figure (c) Output Power

Fig.15 the results of simulation of P&O and IC MPPT algorithms

4.4 Comparison of P&O and IC MPPT Algorithms

The P&O and IC MPPT algorithms are activated and compared under identical conditions (25oC and 1000 W/m2). Table 4 shows the results of the comparison of P&O and IC MPPT algorithms.

Table 4 Comparison of P&O and IC algorithms for Thevenin equivalent model

MPPT	Output Voltage	Output Current	Output Power	Ripple Voltage	Accuracy
P&O	47.522	3.658	173.891	0.29	Less
IC	49.346	3.803	187.661	0.175	Accurate

The American Journal of Engineering and Technology
(ISSN – 2689-0984)
VOLUME 04 ISSUE 04 Pages: 17-35
SJIF IMPACT FACTOR (2020: 5. 32) (2021: 5. 705) (2022: 6. 456)
OCLC – 1121105677 METADATA IF – 7.856
Publisher: The USA Journals

CONCLUSION

In this paper, the single diode and Thevenin equivalent models were used to compare two MPPT algorithms, P&O and IC. The two algorithms are discussed, and the results of their simulations are shown. For both models, it is demonstrated that the Incremental conductance approach outperforms the P&O strategy. The two MPPT algorithms obtained higher output power using single diode model in comparison with the Thevenin equivalent model. The output voltage ripple in the IC algorithm is less when Thevenin equivalent model is used. Both tracking methods improve the photovoltaic system's dynamics and steady-state performance, in addition to the effectiveness of the dc-dc converter system.

REFERENCES

1. D. P. Hohm, M. E. Ropp, "Comparative Study of Maximum Power Point Tracking Algorithms Using an Experimental, Programmable, Maximum Power Point Tracking Test Bed", Conference Record of the Twenty-Eighth IEEE Photovoltaic Specialists Conference, 15-22 Sept. 2000, pp. 1699-1702.
2. A. Ismael Nusaif and A. Lateef Mahmood, "MPPT Algorithms (PSO, FA, and MFA) for PV System under Partial Shading Condition, Case Study: BTS in Algazalia, Baghdad", INTERNATIONAL JOURNAL of SMART GRID, Vol.4, No.3, September, 2020.
3. Bahaa Abdulkhailq Numan, Amina Mahmoud Shakir, Anas Lateef Mahmood," Photovoltaic array maximum power point tracking via modified perturbation and observation algorithm", International Journal of Power Electronics and Drive System (IJPEDS), Vol. 11, No. 4, December 2020, pp. 2007~2018.
4. Hairul Nissah Zainudin, Saad Mekhilef, "Comparison Study of Maximum Power Point Tracker Techniques for PV Systems," Proc. 14th International Middle East Power Systems Conference (MEPCON"10), Cairo University, Egypt, 2010, 750-755.
5. Trishan Esram, and Patrick L. Chapman, "Comparison of Photovoltaic Array Maximum PowerPoint Tracking Techniques," IEEE Transactions on Energy Conversion, 22 (2), 2007, 439-449.
6. D. Haji and N. Genc, "Fuzzy and P&O Based MPPT Controllers under Different Conditions", 7th International Conference on Renewable Energy Research and Applications (ICRERA), Paris, France, pp. 649-655, 14-17 Oct. 2018.
7. H. S. Rauschenbach, "Solar Cell Array Design Handbook". New York: Van Nostrand Reinhold, 1980.
8. M. G. Villalva, J. R. Gazoli, and E. R. Filho, "Modeling and circuit based simulation of photovoltaic arrays," Brazilian Journal of Power Electronics, vol. 14, no. 1, pp. 35 – 45, Feb. 2009.
9. Minwon Park, and In-Keun Yu "A novel real-time simulation Technique of photovoltaic generation systems using RTDS," IEEE Trans. Energy Conversion, vol. 19, no. 1, pp. 164 – 169, Mar. 2004.
10. O. Wasynczuk, "Modeling and Dynamic Performance of a Line-Commutated Photovoltaic Inverter System," IEEE Review, Power Engineering, vol. 9, no. 9 pp. 35 – 36, Sep. 1989.
11. S. Rahman, and B. H. Chowdhury, "Simulation of photovoltaic power systems and their performance prediction," IEEE Trans.Energy conversion, vol. 3, no. 3, pp. 440 – 446, Sep. 1988.
12. B. Galiana, C. Algora, I. Rey-Stolle, and I. G. Vara, "A 3-Dmodel for concentrator solar cells based on distributed circuit units," IEEE Trans. Electron Devices, vol. 52, no. 12, pp. 2552– 2558, Dec, 2005.

The American Journal of Engineering and Technology
(ISSN – 2689-0984)
VOLUME 04 ISSUE 04 Pages: 17-35
SJIF IMPACT FACTOR (2020: 5. 32) (2021: 5. 705) (2022: 6. 456)
OCLC – 1121105677 METADATA IF – 7.856
Publisher: The USA Journals

13. Yun Tiam Tan, D. S. Kirschen, and N. Jenkins, "A model of PV generation suitable for stability analysis," IEEE Trans. Energy Conversion, vol. 19, no. 4, pp. 748 – 755, Dec. 2004.
14. J. T. Bialasiewicz, "Renewable Energy Systems With Photovoltaic Power Generators: Operation and Modeling," IEEE Trans. Industrial Electronics, vol. 55, no. 7, pp. 2752 – 2758, Jul. 2008.
15. M. Rashid, "Power electronics handbook", Academic Press, Canada, 2001.
16. Ray-Lee Lin, and Yi-Fan Chen "Equivalent Circuit Model of Light-Emitting-Diode for System Analyses of Lighting Drivers," Industry Applications Society Annual Meeting 2009, pp. 1–5
17. D. Hohm and M. Ropp, "Comparative study of maximum power point tracking algorithms using an experimental, programmable, maximum power point tracking test bed", IEEE Photovoltaic Specialists Conference, Anchorage, September 2000.
18. C. Liu, B. Wu and R. Cheung, "Advanced algorithm for MPPT control of photovoltaic systems", Canadian Solar Buildings Conference, Montreal, August 2004.
19. D. Hohm and M. Ropp, "Comparative study of maximum power point tracking algorithms using an experimental, programmable, maximum power point tracking test bed", IEEE Photovoltaic Specialists Conference, Anchorage, September 2000.
20. K. Hussein, I. Muta, T. Hoshion and M. Osakada, "Maximum photovoltaic power tracking: an algorithm for rapidly changing atmospheric conditions", IEE Proceedings Generation, Transmission and Distribution, Vol. 142, No. 1, PP: 59-64, January 1995.